"A Cochlear Nucleus Auditory prosthesis based on microstimulation"

Contract No. **No. NO1-DC-1-2105**
Progress Report #8

HUNTINGTON MEDICAL RESEARCH INSTITUTES
NEURAL ENGINEERING LABORATORY
734 Fairmount Avenue
Pasadena, California 91105

D.B. McCreery, Ph.D.
A.S. Lossinsky, Ph.D.
L.A. Bullara, B.S.

HOUSE EAR INSTITUTE
2100 WEST THIRD STREET
Los Angeles, California 90057

R.V. Shannon Ph.D
S. Otto M.S.
M. Waring, Ph.D

SUMMARY & ABSTRACT

The objective of this project is to develop central auditory prostheses based on an array of microelectrodes implanted into the ventral cochlear nucleus, in order to restore hearing to patients in whom the auditory nerve has been destroyed bilaterally. Our contract calls for the development of arrays of silicon substrate electrodes, which should allow placement of many more electrode sites into the human cochlear nucleus than is possible with discrete iridium microelectrodes. We are developing an array for implantation into the human cochlear nucleus which has 16 electrode sites distributed on 4 silicon shanks extending from an epoxy superstructure that is 2.4 mm in diameter.

Cat CN142 was maintained for 63 days after implanting an array of 4 silicon substrate shanks and 16 simulating electrodes sites into the posteroventral cochlear nucleus. At autopsy, it was determined that the two rostral silicon shanks were within the PVCN. The histologic evaluation of the implant site suggests some loss of neurons within 50 μm of the silicon shanks, but the thresholds of the potentials evoked from all of the microelectrode sites in the PVCN stabilized after approximately 42 days in vivo, at values comparable to what we had previously measured for discrete iridium microelectrodes implanted chronically in the PVCN.

At 63 day after array implantation, the ability of the ensemble of microelectrode sites to access the tonotopic organization of the PVCN was evaluated by recording the compound action potentials evoked from each of the microelectrode sites, at a sequence of depths along the dorsolateral-ventromedial axis of the contralateral IC. By using current source-density analysis, it was shown that the ensemble of microelectrode sites was able to excite separate populations of neurons in the PVCN, and was able to access the tonotopic organization of the PVCN in an orderly manner. This was determined by current density analysis of the serial depth recordings made in the contralateral inferior colliculus.

METHODS

The objective of this project is to develop central auditory prostheses based on an array of microelectrodes implanted into the ventral cochlear nucleus, in order to restore hearing to patients in whom the auditory nerve has been destroyed bilaterally. Our contract calls for the development of arrays of silicon substrate electrodes, which should allow placement of many more electrode sites into the human cochlear nucleus than is possible with discrete iridium microelectrodes. We are developing an array for implantation into the human cochlear nucleus that has 16 electrode sites distributed on 4 silicon shanks extending from an epoxy superstructure that is 2.4 mm in diameter. This is the same footprint as our first- generation human arrays employing discrete iridium microelectrodes and is designed to be implanted using the same inserter tool. The silicon probes are fabricated at the University of Michigan under the direction of Design Engineer Jamille Hetke.

The probe shanks are either 2 or 3 mm in length. The 3 mm probes are intended to span the full tonotopic gradient of the human ventral cochlear nucleus. The 2 mm shanks are appropriate for implantation into the feline ventral cochlear nucleus. Figure 1 shows a probe with 2 of the 2 mm shanks, each with four 2,000 μm^2 iridium electrode sites distributed between 0.8 and 1.7 mm below the horizontal spine. A stainless-steel pin is affixed to the rear of the probe, and embedded in a backing of EpoTek 301 epoxy. The pin is used in the handling of the probes and to align the probe shanks when the probe is incorporated into an array. After the pin and the EpoTek backing are applied to the rear of the horizontal spine, the electrical lead wires are bonded to the pads on the spine, and the junctions are insulated with Nusil 4211 silicon elastomer, as shown in Figure 1. Figure 2 shows an array with 2 of the probes (4 shanks and 16 sites) extending from an epoxy (EpoTek 301) superstructure which floats on the dorsal surface of the cochlear nucleus. The array cable is angled vertically, to accommodate the transcerebellar approach to the feline cochlear nucleus.

We have been experiencing a problem with our probes wherein some of the electrode sites become non-functional(open-circuited) at some stage during the fabrication process. We have traced this to fracturing of the silicon spine when the alignment pin is removed from the array near the end of the fabricating process. We appear to have solved this problem, by modifying the process by which the pin is attached to the rear surface of the probe; the new procedure entails placing a thin cushion of silicon elastomer between the pin and the probe spine.

The surgical implantation of the arrays into the feline ventral cochlear nucleus was described in QPR#7. Using general anesthesia and aseptic technique, a small craniectomy was made over the left lateral cerebellum just posterior to the tentorium. The rostro-lateral portion of the cerebellum was aspirated using small pipettes, to expose the dorsal surface of the cochlear nucleus. The upper surface of the array's epoxy superstructure was positioned on the end of a vacuum wand mounted on a stereotaxic electrode carrier and advanced into the dorsolateral surface of the cochlear nucleus. The recording electrode was inserted by stereotaxis into the extreme rostral end of the right inferior colliculus, in order to broadly sample inputs from the cochlear nucleus. The recording reference electrode was implanted dorsal to the right inferior colliculus.

Cat CN142 was followed for 63 days after implanting the electrode array. At 15, 24, 42 and 63 days after implantation, the cat was anesthetized lightly with Propofol and the responses evoked from each of the microelectrodes in the left PVCN were recorded via the electrode in the rostral pole of the right inferior colliculus. The stimulus was cathodic-first, charge-balanced pulse pairs, each phase 150 μs in duration. 1024 successive responses were averaged to obtain each averaged evoked response (AER, Figure 3). Because of its short (~ 1 ms) latency after the stimulus, the 1st component of the AER shown in Figure 3 is assumed to represent neuronal activity evoked directly in the neurons projecting from the PVCN to the

inferior colliculus, while the second component may represent neuronal activity that is evoked transsynaptically. The response growth functions, which represent the recruitment of the neural elements surrounding the microelectrode, were generated for each stimulating electrode site in the PVCN, by plotting the amplitude of the first component of each of the AERs evoked from the site, against the amplitude of the "probe" stimulus that evoked the AER.

Figure 4 shows the location of each of the electrode sites on the array implanted into cat CN142. The response growth functions were measured over a range of current amplitudes, between 0 and 35 μA. The amplitude of the response evoked in the inferior colliculus by a stimulus or 35 μA is similar to that evoked by an acoustic click with a mean sound pressure of approximately 55 DB.

After recording the response growth functions on the 63 day, an experiment was conduced to determine the capacity of the silicon array to access the tonotopic gradient of the PVCN. We used an approach similar to the one employed previously to demonstrate that discrete microelectrodes could access the tonotopic gradient of the PVCN in an orderly manner (McCreery et al, 1998). The cat was transitioned to Halothane-nitrous oxide anesthesia and its head mounted in the stereotaxic frame. The inferior colliculus contralateral to the microstimulating array was exposed by aspirating the occipital pole of the right cerebral hemisphere. An iridium recording electrode with an exposed surface area of approximately 10,000 μm^2 was advanced into the colliculus at an angle of 45^O above the horizontal. The responses evoked by pulsing each of the microelectrode sites at an amplitude of 30 μA (150 μs/phase) was recorded at interval of 200 μm along the dorsolateral-ventromedial axis of the central nucleus of the IC, which is approximately along the tonotopic axis of the colliculus (Brown et al, 1997, Harris 1987).

Current source density (CSD) analysis has been shown to be useful for localizing coherent induced neural activity. The technique locates regions within the tissue volume in which current is passing from the extracellular compartment into (or out of) a spatially extensive intracellular compartment. The latter might be myelinated axons or the apical dendrites of large neurons. The CSD at point x,y,z within the tissue volume represents the net current flowing in or out of the neural elements and is given by:

$$I_{d(x,y,z)} = -[\ \sigma_x\ \delta^2\ \phi/\delta x^2 + \sigma_y\ \delta^2\ \phi/\delta y^2 + \sigma_z\ \delta^2\ \phi/\delta z^2\ ] \qquad (1)$$

where ϕ is the field potential at x,y,z, and σ_x, σ_y and σ_z are the principal tissue conductances (Freeman and Nicholson, 1975). To compute equation 1, the extracellular field potential must be measured simultaneously at 7 (or more) points, at and around x,y,z. However, in situations in which the neuronal responses to the stimulation are quite constant over time and in which the tissue is nearly isotropic ($\sigma x \cong \sigma y \cong \sigma z \cong \sigma$) as in the central nucleus of the inferior colliculus (Harris, 1987), then the current source density can be computed from measurements of the averaged evoked potential obtained along a single axis. Freeman and Nicholson (1975) compared various smoothing procedures for reducing the noise inherent in the calculation of the 2nd spatial derivative of ϕ, while maintaining the essential spatial resolution: . The 5-point finite approximation appeared to be the most useful:

$$I_{d(x,y,z),} \cong D(x,y,z) = (0.01\ \sigma/h^2)[-2\phi(x-2h) - \phi(x-h) - 2\phi(x) + \phi(x+h) + 2\ \phi(x+2h)] \qquad (2)$$

Here, h is the spacing between the points at which the instantaneous field potential ϕ is measured. This formula is computationally equivalent to obtaining a least-squares error fit of a cubic polynomial to 5 successive data points along the axis of measurement, and then computing the second derivative of the fitted polynomial. We did not measure the conductivity of the living tissue in the inferior colliculus, and therefore, the CSD is expressed as arbitrary

units.

At the end of the experiment, the cat was deeply anesthetized with pentobarbital, given i.v. heparin and perfused through the aorta for 1 minutes with a prewash solution consisting of 90 ml of phosphate-buffered saline, and 0.05% procaine HCl. This was followed by a fixative containing 4% formalin and 0.25% glutaraldehyde in 0.1 M sodium phosphate buffer. The microelectrode array was removed from the left cochlear nucleus after dissection of the overlying connective tissue. The tissue block containing the cochlear nucleus was removed and washed overnight in 4% formalin, then in distilled water for 2 hrs, dehydrated in a graded series of ethanol and embedded in paraffin. The paraffin-embedded tissue block was cut at a thickness of 6-7 μm and the sections picked up on histogrip-coated-slides. These slides were routed either for routine histologic staining with Nissl stain (Cresyl violet), or for NeuN immunohistochemistry. The monoclonal antibody to NeuN (mAb A60) has been shown to bind selectively to proteins within the nucleus (primarily) and cytosol of neurons of the CNS of humans, rats, mice, chickens, ferrets and salamanders (Mullen et al, 1992. The tissue sections were processed using an antigen retrieval method, as described by Wolf et al (1996).

RESULTS

Cat CN142 was maintained for 63 days after implanting the microelectrode array in the left posteroventral cochlear nucleus (PVCN). At autopsy, it was determined that only the two rostral silicon shanks were within the PVCN. Figure 5A,C,E show the response growth functions (RGFs) of the early component of the response evoked in the contralateral Inferior colliculus (IC), for the 4 electrode sites on the rostral-lateral shank, at 15, 42 and 63 days after implantation. Figure 5B,D,F show the corresponding data for the 3 functional sites on the rostral-medial shank. Between the 15th and 42nd day, the threshold of the evoked response increased from <5 -10 μA, to ~ 5-15 μA. The slope of all of the RGFs also decreased, but that change might be due to the ongoing encapsulation of the recording electrode deep in the rostral pole of the IC. Between the 42nd and 63rd day, the thresholds and slopes of the RGFs were very stable.

On the 63rd day, the ability of the ensemble of microelectrode sites to access the tonotopic organization of the PVCN was evaluated by recording the compound action potentials evoked from each of the microelectrode sites, at a sequence of depths along the dorsolateral-ventromedial axis of the contralateral IC. It is well established that high and low acoustic frequencies from the basal and apical cochlea map onto a dorsal-to-ventral tonotopic gradient in the PVCN, and that this ordered representation of acoustic frequencies then projects (in an inverted manner) onto the central nucleus of the IC, with low acoustic frequencies represented in the dorsolateral part of the IC's central nucleus (Figure 6).

Figure 7A,B show families of potentials evoked from two of the microelectrodes sites (#5 and #13) in the left PVCN and recorded along the DL-VM axis of the right IC. The numbers to the right of each trace designate the depth of the recording below the surface of the IC. The responses were evoked by a stimulus of 30 μA, which is near the maximum of the range used to generate the RGFs shown in Figure 5. Figure 8 shows plots of the peak-to-peak amplitude of the large component with a latency of ~ 4 ms after the stimulus pulse pair (indicated by the arrows in Figure 7), for the 4 electrodes sites on the rostral-lateral probe shank. Figure 9A,B show the magnitude of the current sink density for the 7 functional electrodes sites on the rostral-lateral and rostral-medial shanks, for the same response component. The current sink density was computed using equation(2) from METHODS. In Figure 7A, the peaks of the current density plots are quite well separated, indicating that each electrode site in the PVCN was exciting a population of neurons that were at least partly distinct. The microelectrode sites that were most shallow (more dorsal) in the PVCN induced neuronal activity deepest in the IC and

the entire sequence was ordered according to the know organization of the tonotopic projection from the PVCN to the IC. Figure 7B shows the plots of the current sink density for the three functions electrodes sites on the rostral-medial shank of the simulating array. The current sink for adjacent electrode sites 6 and 10 did not show the expected separation with depth in the IC, but the neural activity induced by the most ventral site (# 14) was more dorsal in the IC than the activity induced by either of the more dorsal simulating sites, #6 and #10. Collectively, the neural activity induced by the 7 functional sites on the two shanks spanned most of the depth of the central nucleus of the IC.

At the end of the mapping study, the cat was perfused for histologic evaluation of the implant site. The superstructure of the chronically-implanted array was encapsulated in connective tissue and while freeing and removing the array, the rostral-medial silicon shank fractured from the superstructure and remained impaled in the tissue. The fractured shank was left *in situ* during tissue processing and sectioning of the paraffin-embedded tissue.

Figure 10A shows a Nissl-stained section through a portion of both shanks, and approximately parallel to the shanks. The rostral-lateral shank (rl) had penetrated into the lateral portion of the PVCN. The fragments of the silicon shank are visible within the lumen of the medial shank (rm). Figure 10B shows a nearby section that was stained for the neuron-specific antigen NeuN, and counter-stained for Nissl. Neurons are seen within approximately 50 μm of both tracks. However, it does appear that there was a reduction in the spatial density of neurons very close to both of the shanks, and this may account for the increase in the threshold of the response growth functions between the 15th and 42nd day after implantation of the array. Also, there is a glial scar, approximately 75 μm in width, medial to the tip of the lateral shank (Figure 10C).

In summary, we have demonstrated the feasability of chronically implanting an array of silicon-substrate microprobes into the feline ventral cochlear nucleus. The histologic evaluation of the implant site suggests some loss of neurons very close to the silicon shanks, but the threshold of the potentials evoked from all of the microelectrode sites stabilized after approximately 42 days *in vivo,* at values comparable to what we had previously measured for discrete iridium microelectrodes implanted chronically in the PVCN (McCreery et al, 2000). After 63 day, the ensemble of microelectrodes was able to access the tonotopic organization of the PVCN in an orderly manner, as determined by current density analysis of the serial depth recordings in the contralateral inferior colliculus.

REFERENCES

1. Freeman, J. A., and C. Nicholson. Experimental optimization of current source-density technique for anuran cerebellum. *J Neurophysiol* 38: 369-82., 1975.
2. Harris, D. M. Current source density analysis of frequency coding in the inferior colliculus. *Hear Res* 25: 257-66, 1987.
3. Ryan, A. F., J. M. Miller, Z. X. Wang, and N. K. Woolf. Spatial distribution of neural activity evoked by electrical stimulation of the cochlea. *Hear Res* 50: 57-70., 1990.
4. Mullen, R. J., C. R. Buck, and A. M. Smith. NeuN, a neuronal specific nuclear protein in vertebrates. *Development* 116: 201-211., 1992.
5. Wolf, H. K., R. Buslei, R. Schmidt-Kastner, P. K. Schmidt-Kastner, T. Pietsch, O. D. Wiestler, and I. Bluhmke. NeuN: a useful neuronal marker for diagnostic histopathology. *J Histochem Cytochem* 44: 1167-71., 1996.
6. Brown, M., W. R. Webster, and R. L. Martin. The three-dimensional frequency organization of the inferior colliculus of the cat: a 2-deoxyglucose study. *Hear Res* 104: 57-72., 1997.
7. Harris, D. M., R. V. Shannon, R. Snyder, and E. Carney. Multi-unit mapping of acoustic stimuli in gerbil inferior colliculus. *Hear Res* 108: 145-56., 1997.
8. McCreery, D. B., R. V. Shannon, J. K. Moore, and M. Chatterjee. Accessing the tonotopic organization of the ventral cochlear nucleus by intranuclear microstimulation. *IEEE Trans Rehabil Eng* 6: 391-9, 1998.
9. McCreery, D. B., T. G. Yuen, and L. A. Bullara. Chronic microstimulation in the feline ventral cochlear nucleus: physiologic and histologic effects. *Hear Res* 149: 223-38, 2000.

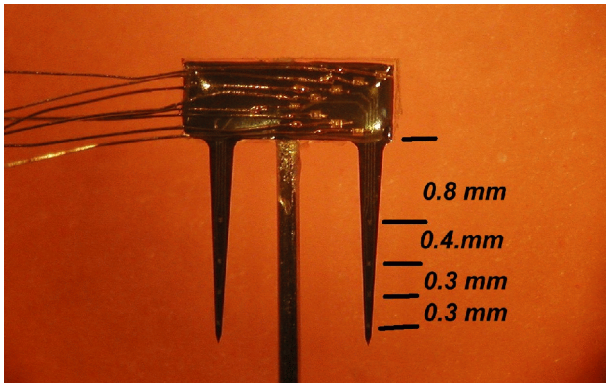

Figure 1

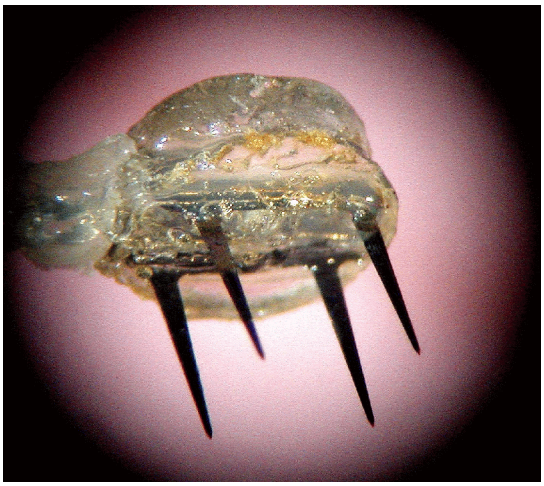

Figure 2

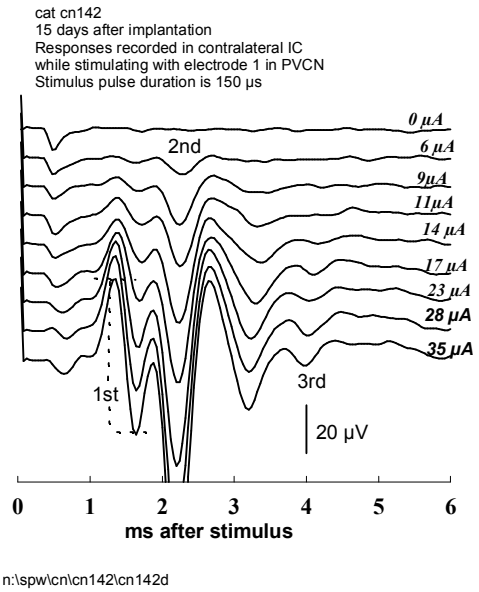

Figure 3

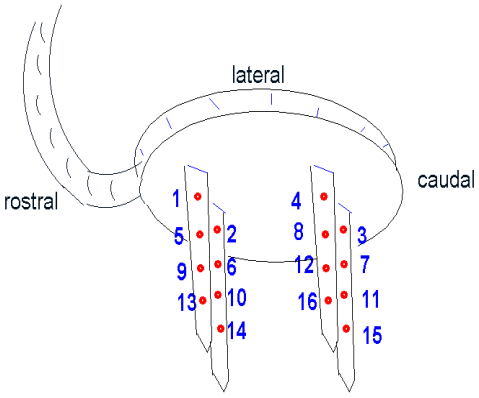

Figure 4

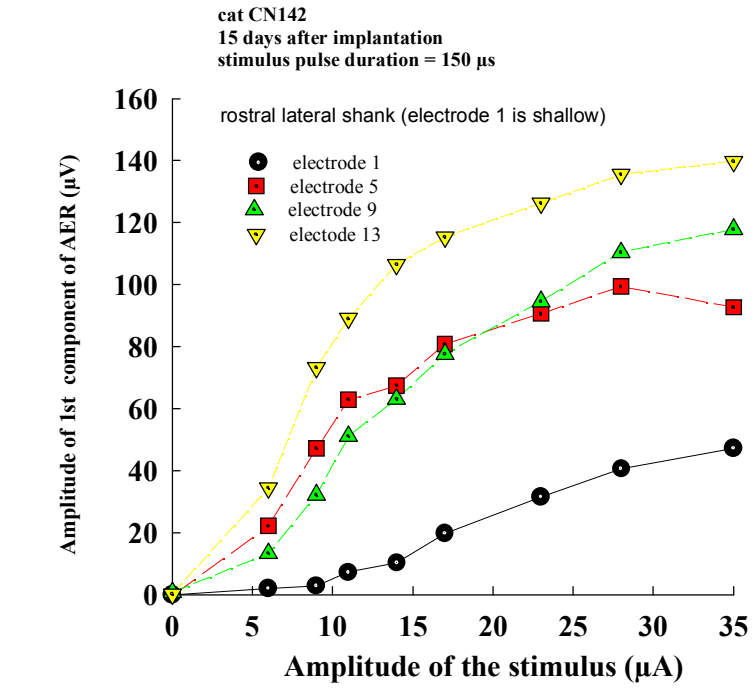

n:\spw\cn\cn142\cn142b.spw

Figure 5A

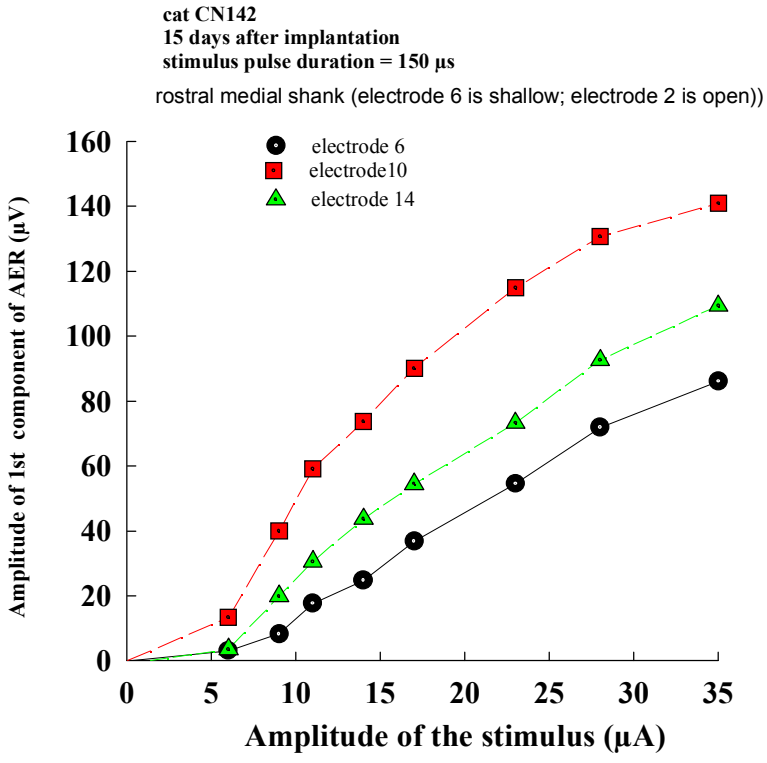

n:\spw\cn\cn142\cn142c.spw

Figure 5B

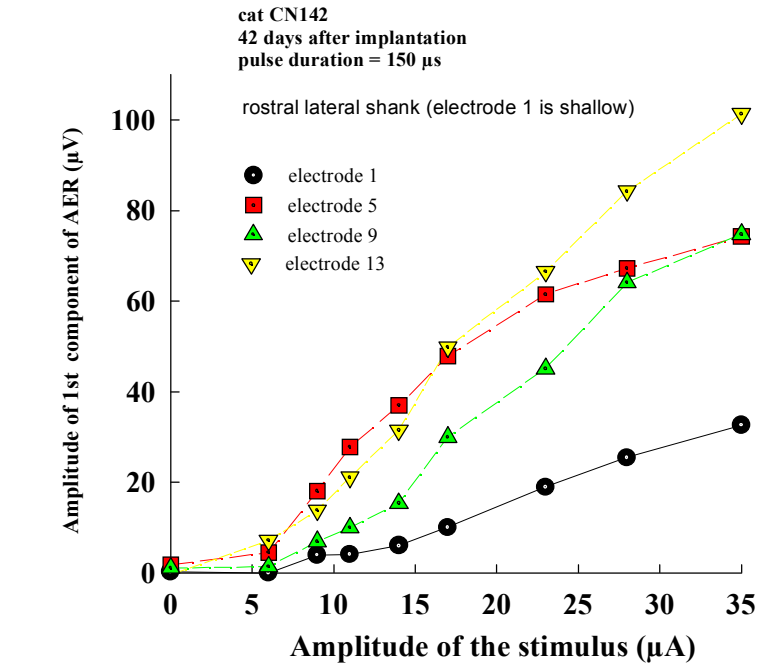

n:\spw\cn\cn142\cn142i.spw

Figure 5C

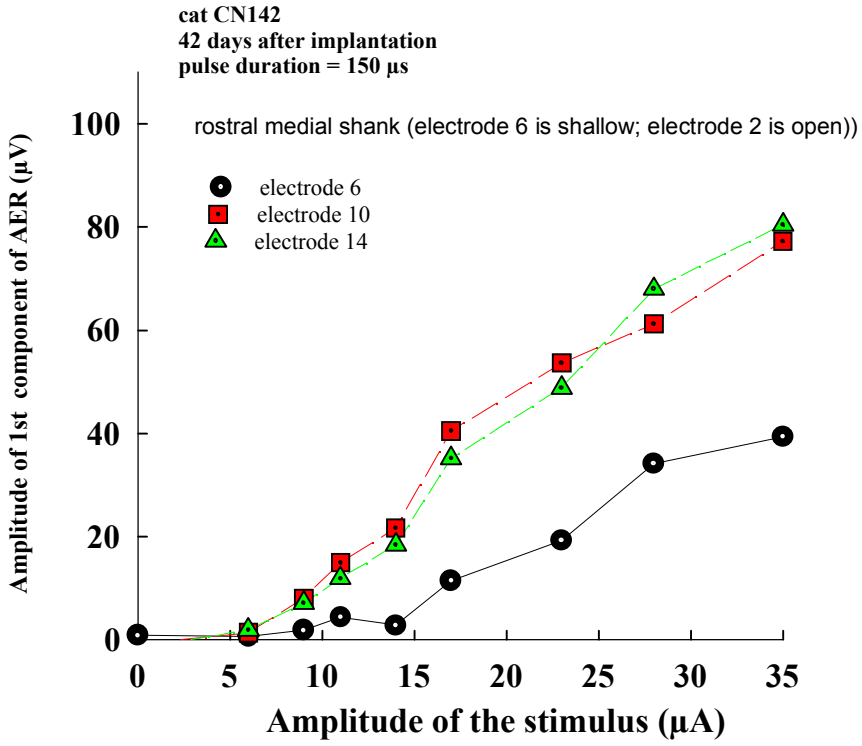

n:\spw\cn\cn142\cn142j.spw

Figure 5D

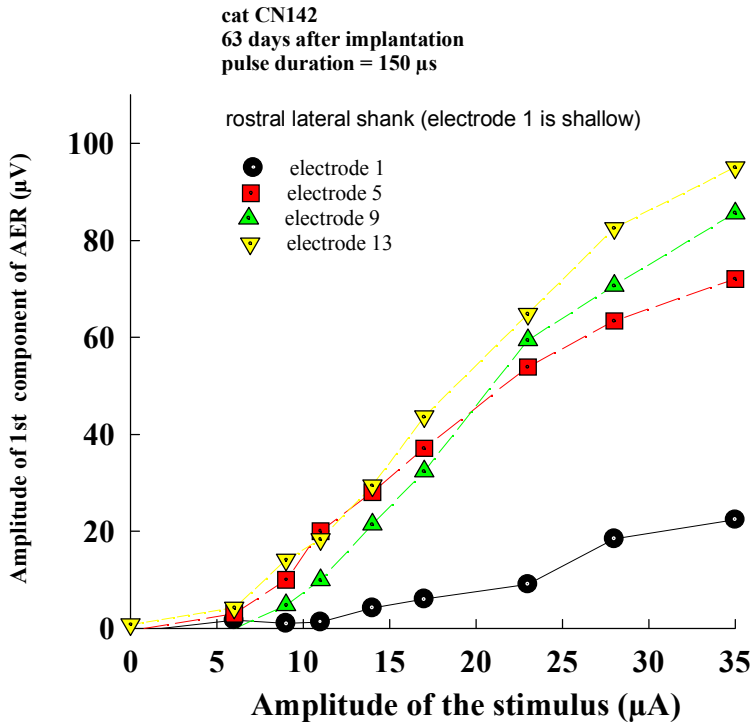

n:\spw\cn\cn142\cn142o.spw

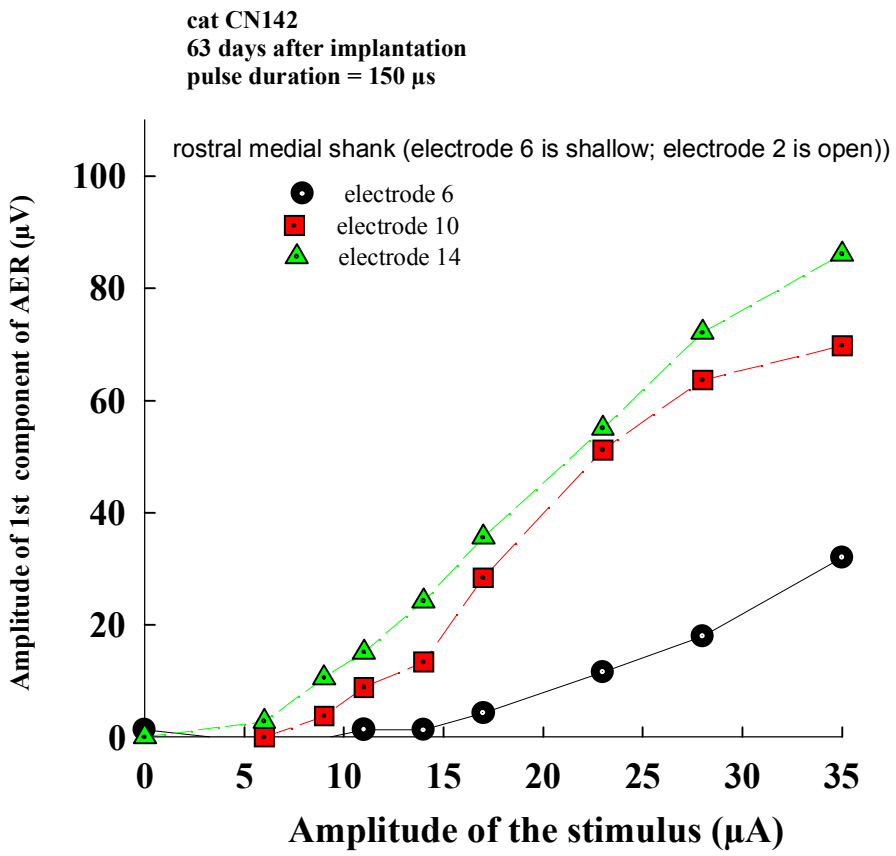

n:\spw\cn\Cn142\cn142p.spw

Figure 5F

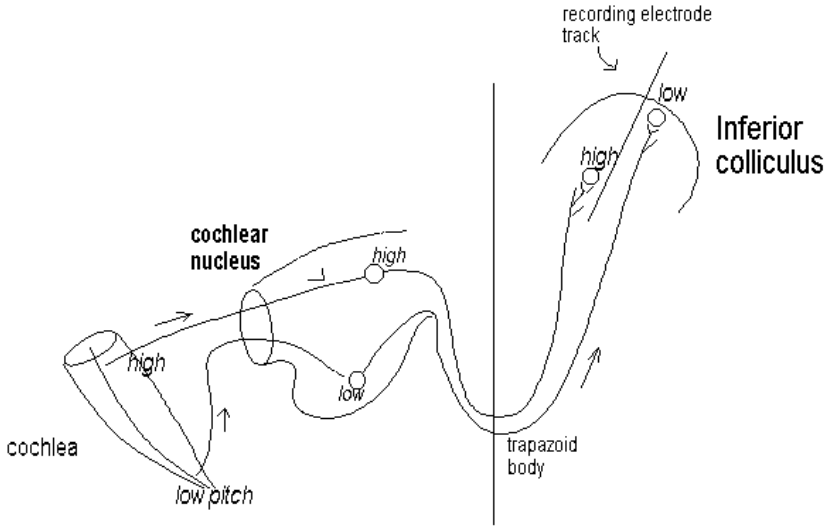

Figure 6

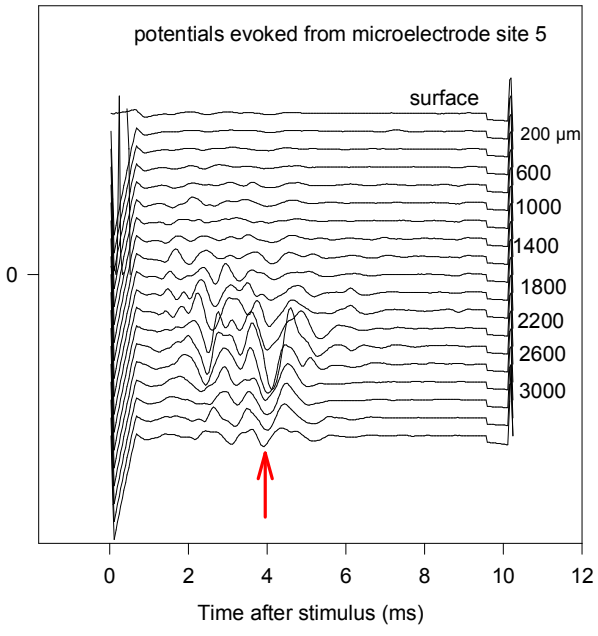

n:\spw\cn\cn142\cn142q

Figure7A

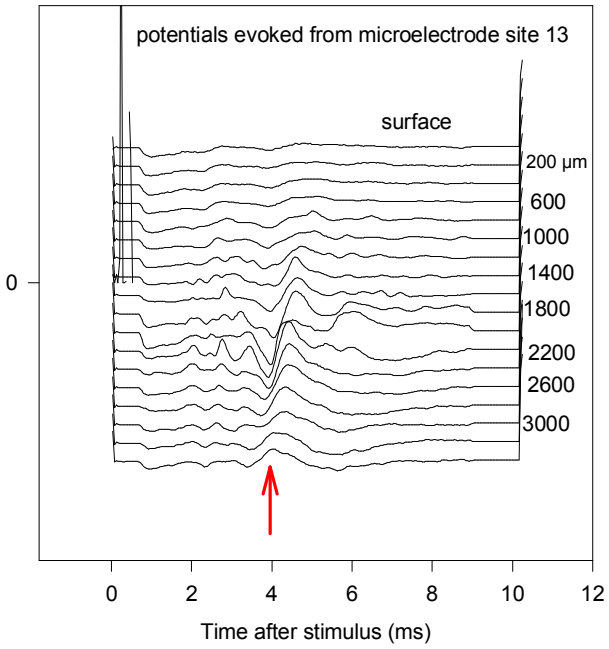

n:\spw\cn\cn142\cn142r

Figure 7B

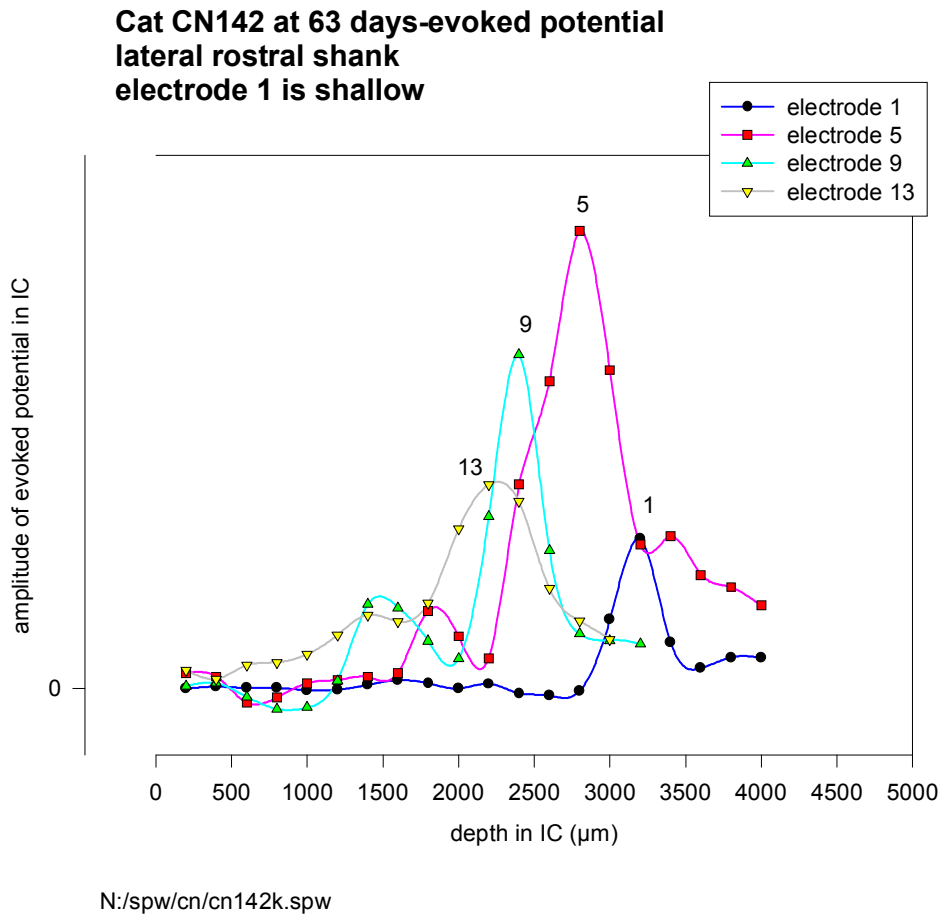
Cat CN142 at 63 days-evoked potential
lateral rostral shank
electrode 1 is shallow
electrode 1
electrode 5
electrode 9
electrode 13
amplitude of evoked potential in IC
0
5
9
13
1
0
500
1000
1500
2000
2500
3000
3500
4000
4500
5000
depth in IC (µm)
N:/spw/cn/cn142k.spw

Figure 8

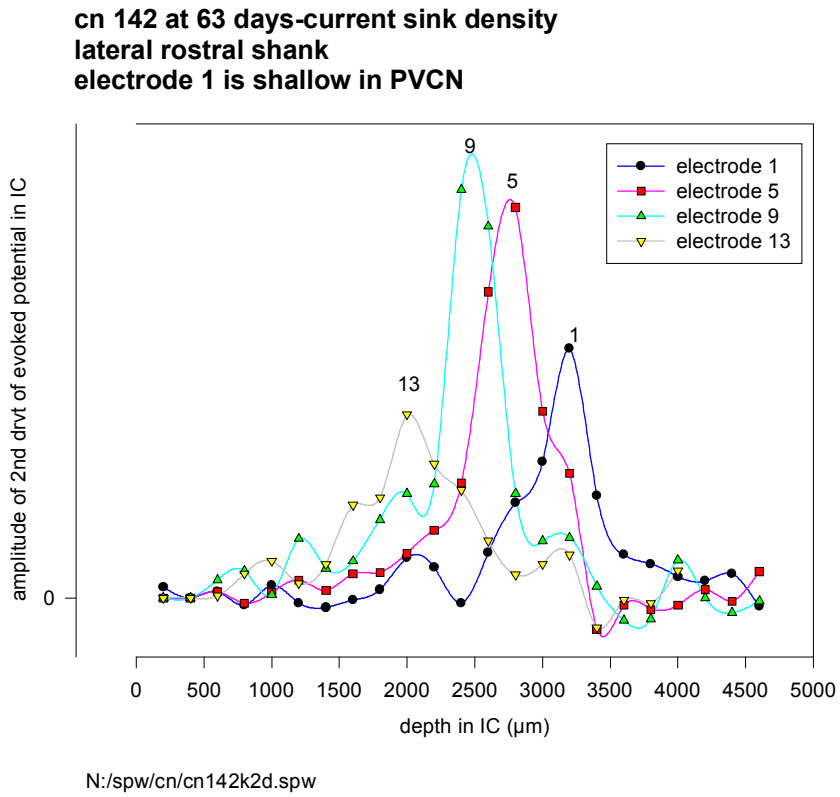

Figure 9A

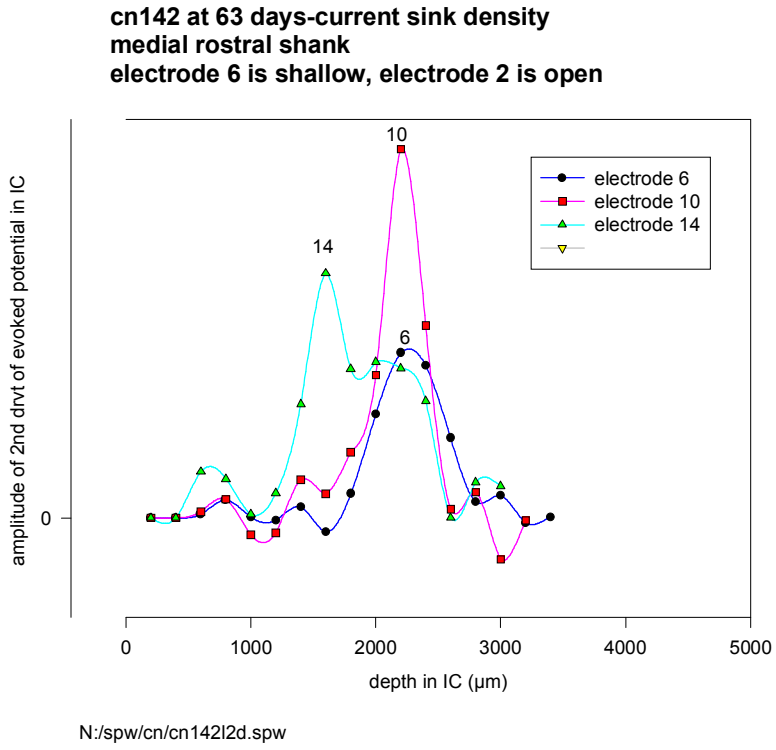

Figure 9B

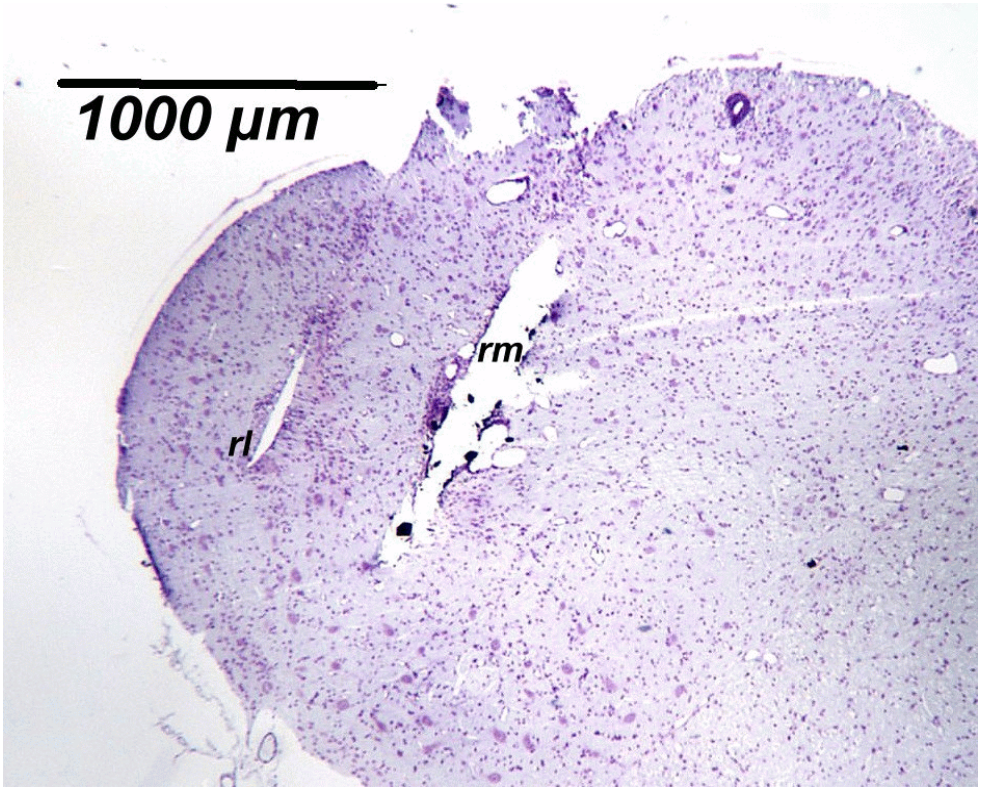

Figure 10A

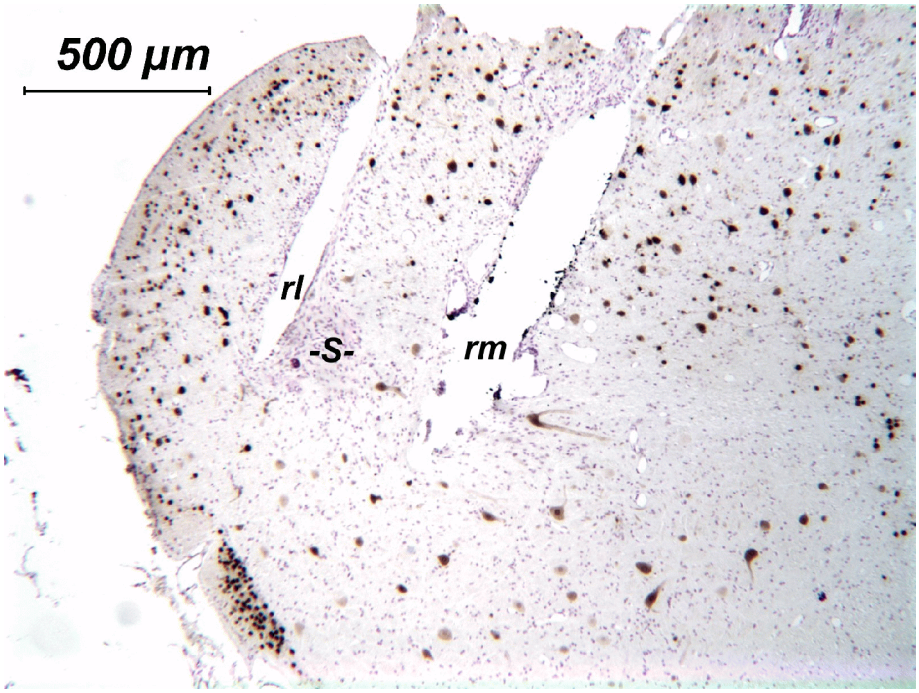

Figure 10B

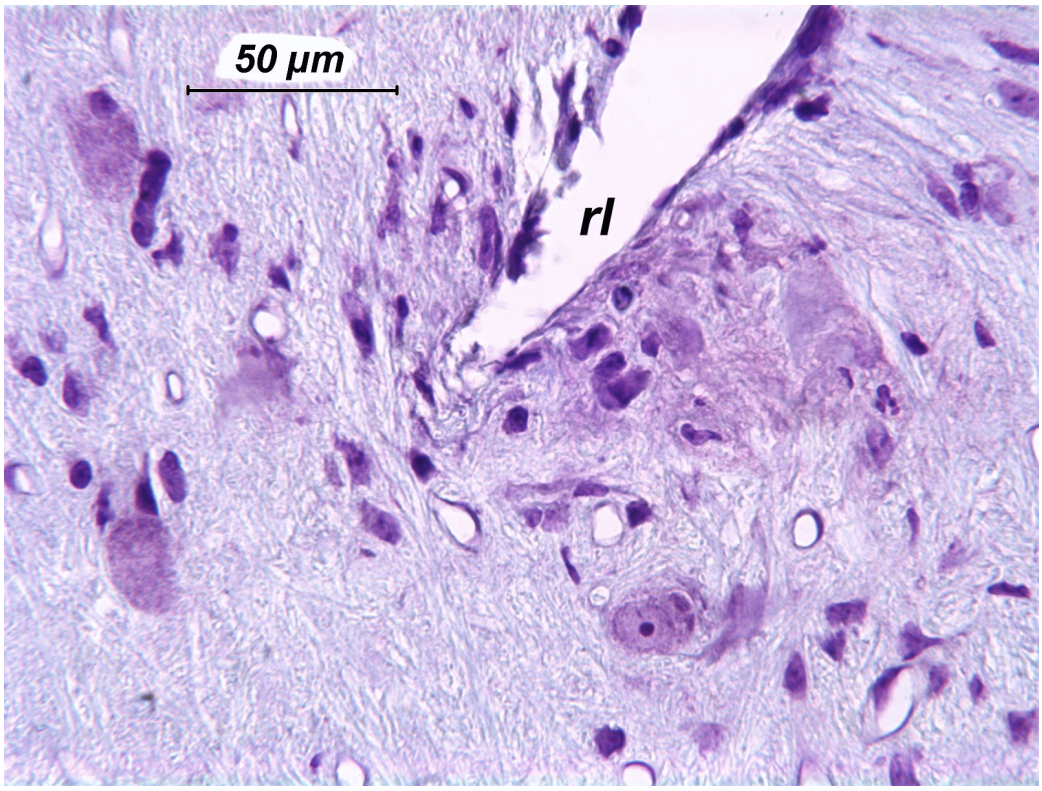

Figure 10C